Ultrasonics 114 (2021) 106369

Contents lists available at ScienceDirect

Ultrasonics

journal homepage: www.elsevier.com/locate/ultras

The fundamental ultrasonic edge wave mode: Propagation characteristics and potential for distant damage detection

James M. Hughes [a,*], Munawwar Mohabuth [a], Andrei Kotousov [a], Ching-Tai Ng [b]

[a] School of Mechanical Engineering, The University of Adelaide, SA 5005, Australia
[b] School of Civil, Environmental, and Mining Engineering, The University of Adelaide, SA 5005, Australia

ARTICLE INFO

Keywords:
Edge waves
Feature-guided waves
Defect monitoring
FEA
Laser Vibrometry

ABSTRACT

Engineering structures are often composed of thin elements containing features such as free edges, welds, ribs, and holes, which makes distant safety inspections based on guided waves difficult due to wave scattering. However, these features can themselves generate so-called 'feature-guided' waves, which can potentially be utilised for damage detection. One such example are flexural wedge waves, which have been investigated extensively both theoretically and experimentally in the past. Another example is edge waves. These waves, which are a natural analogue of Rayleigh waves propagating in a finite thickness plate, have received relatively little attention, specifically with respect to their possible use in distant damage inspections and Structural Health Monitoring systems. The current paper is aimed to address this gap, and it is focused on the investigation of the fundamental mode of edge waves (ES_0), which is the most promising for practical applications. The features of the transient ES_0 mode are investigated experimentally and numerically, and compared with previous theoretical studies. It was demonstrated that the ES_0 mode can be effectively excited with the wedge excitation method, and distant damage detection with this wave mode at low frequency-thickness values (FTV < 5) is readily achievable. In particular, in a laboratory environment the ES_0 mode propagated several meters with almost no decay. However, at higher frequency-thickness values, a wave amplitude modulation, significant energy decay and strong coupling between the ES_0 and S_0 wave modes were observed. These phenomena may restrict the defect resolution as well as the range of damage inspections based on the fundamental edge wave mode.

1. Introduction

Guided waves have many promising applications in the nondestructive evaluation (NDE) of thin-walled structures and, especially, in Structural Heath Monitoring (SHM) [1]. Guided waves, specifically Lamb waves, can propagate over long distances without significant attenuation carrying information about mechanical damage, e.g. discontinuities and local geometry changes caused by impact, fatigue or corrosion [2]. However, the influences of ambient temperature variations, possible changes of loading and boundary conditions, the unavoidable presence of multiple wave modes, and scattering from structural features can make interpretation of the signal information carried by guided waves very difficult [3]. A great deal of research over the past two decades was directed to address these shortcomings with an ultimate objective to increase the reliability of damage detection and the sensitivity to various types of mechanical damage [4,5].

The generation of higher-order guided wave modes can be avoided by limiting the excitation frequency below the first cut-off frequency and utilising appropriate excitation methods, such as the wedge excitation method, which aims to direct energy from a transducer into the desired propagation direction and wave mode(s). Various temperature compensation techniques have also been proposed to address the detrimental effects due to ambient temperature variations [4–6]. It was demonstrated that similar techniques can be applied to compensate for changing loading (stress) conditions [7], because the stress has a similar influence as temperature on wave speeds [8]. However, the effect of various structural features, which are potential sources of wave scattering, is the most challenging issue in the implementation of guided wave based methods in real world applications. This issue was largely addressed with numerical and experimental approaches, which were developed for specific geometries of structural components and types of defects [9–12].

Structural features, such as free edges, welds, ribs, and holes, are not only potential sources of scattering, they also can act as a waveguide

* Corresponding author.
E-mail address: james.m.hughes@adelaide.edu.au (J.M. Hughes).

https://doi.org/10.1016/j.ultras.2021.106369
Received 4 February 2020; Received in revised form 19 December 2020; Accepted 20 December 2020
Available online 11 February 2021

[13,14]. Waves which propagate along these structural elements are often called 'feature-guided' waves, and can potentially be utilised for damage detection near or along structural features. From a structural integrity point of view, various structural features usually represent the critical locations – or hot spots – due to pre-existing fabrication defects, residual stress, and/or stress concentration. Therefore, feature-guided waves represent a great interest in NDE and SHM areas.

Over the past two decades, numerical methods have become very popular in the investigation of guided wave propagation features. In particular, the Semi-Analytical Finite Element (SAFE) method has been applied in a number of recent studies to investigate the mode shapes and dispersion curves of waves guided by features. Yu et al. [15] used the SAFE method to study the modal characteristics of an ultrasonic wave guided by a 90° bend in a composite plate. The results of the numerical analysis were supported by an experimental study, which demonstrated a good agreement with both the SAFE method and 3D FEM results. Waves guided by a weld have also been investigated using the SAFE and experimental methods in [16,17]. One particularly promising potential application of the feature guided waves is identification of de-bonding damage in composites. Yu et al. [18] suggested that a shear-horizontal-like mode with low dispersion and attenuation characteristics could be useful for the evaluation of de-bonding and de-lamination damage in stiffened composite plates.

The so-called wedge waves, which are a kind of feature-guided wave, have received considerable attention over the past decades and have been investigated both theoretically and experimentally. The wedge wave represents a flexural wave mode guided by the apex of a wedge. These waves are non-dispersive in the case of ideal wedge geometry and have a relatively low speed, which make these waves very attractive for damage detection purposes. In addition, it was shown that specific wedge geometries can trap vibrations, acting as an 'acoustic black hole' [19]. This phenomenon can be utilised in vibration control and damping.

The potential of anti-symmetric flexural wedge waves for damage detection within relatively short distances (~100 mm) has been recently demonstrated by Chen et al. [20] and Corcoran et al. [21]. However, wedge waves are very sensitive to the sharpness of the wedge, which gives rise to significant attenuation [22,23]. This may limit their practical usefulness, as it is unrealistic to assume that common structural components have absolutely sharp (null tip) wedges to allow the propagation of non-dispersive wedge waves. A more realistic scenario is a plate with a free edge, which is slightly rounded toward the lateral surfaces. Such geometries allow the propagation of a different type of feature-guided waves – edge waves, which is the focus of the current paper.

Transient guided edge waves are a natural analogue of surface (Rayleigh) waves, which were first studied by Rayleigh in 1885 [24]. Edge waves are guided by the apex of a plate and the wave energy is concentrated near the free surface, similar to wedge waves, meaning they are not subjected to spatial dispersion. However, in contrast to wedge waves, their edge analogue is energy dispersive, and may decay with propagation distance [25,26]. The decay properties of edge waves as well as other guided wave modes are essential for the development of damage detection techniques, especially for correctly selecting the sensor density or setting threshold values for reflected signals in the case of distant defect detection. These properties are yet to be investigated experimentally. Some limited theoretical studies indicate that the attenuation of symmetric edge wave modes increases with the excitation frequency, plate thickness, and Poisson's ratio of the material [25–28].

Edge waves were first experimentally observed by Shaw in 1956 on vibrating thick barium titanate disks [29]. The first explanation of this phenomenon was given by Gazis and Mindlin in 1960, who demonstrated that there exists an infinite spectrum of edge wave modes [30]. There were several detailed theoretical and experimental studies on edge resonance, which is a special case of edge waves with zero wavenumber along the edge direction [26]. In contrast, few investigations have focused on transient edge waves, which were previously considered as an undesirable phenomenon inevitably accompanying the excitation of Lamb waves, and negatively impacting the defect detection capabilities of Lamb wave-based SHM techniques. One exception is a recent study focusing on transient edge waves excited by a flat piezoelectric transducer bonded to the edge of a thick elastic plate [27]. Wave propagation and dispersion at a relatively low frequency-thickness values (FTVs) were investigated with a standard Fourier transform revealing a quite complicated system of interacting waves, which would be very challenging to implement in practical damage detection. Moreover, the propagation distances were limited to 100–150 mm, which is far smaller than the typical distances required for distant damage inspections and SHM applications. The latter becomes economically viable when one sensor covers about 1 m of the structure, as discussed in [31] and other papers.

The aims of this paper are therefore to achieve efficient excitation of the fundamental edge wave mode (ES_0), investigate numerically and experimentally the propagation features of the ES_0 mode over larger distances, and explore the possibility of distant damage detection with this wave mode for the purpose of NDE and SHM. This paper is structured as follows: Section 2 presents a summary of theoretical results obtained based on three-dimensional (3D) linear elastic theory. Section 3 describes the wedge excitation technique and details of the experimental set up and measurement procedures. Section 4 outlines the numerical studies, which complement the experimental results obtained on the free surfaces of the plate. The outcomes of the experimental study are presented in Section 5, along with a comparison with previous theoretical results and the finite element simulations. A demonstration of defect detection utilising the ES_0 mode at a low FTV is also included in this section. Conclusions and possible future developments are discussed in Section 6.

2. Edge waves fundamentals

The mathematical formulation leading to the solution describing edge waves comprises the 3D equations of linear elasticity, which can be written in terms of displacement vector $\boldsymbol{u} = (u_1, u_2, u_3)$ [24–28]:

$$(\lambda + \mu)\text{grad div}\boldsymbol{u} + \mu\Delta\boldsymbol{u} = \rho\ddot{\boldsymbol{u}} \tag{1}$$

for a domain $V = (|x_1| < \infty, |x_2| \le h, -\infty < x_3 \le 0)$ representing a semi-infinite plate. In Eq. (1) λ, μ and ρ are Lame constants and the mass density, and Δ is the three-dimensional Laplace operator, $\ddot{\boldsymbol{u}} = \partial^2\boldsymbol{u}/\partial t^2$. Traction free boundary conditions are enforced on two plate faces ($x_2 = \pm h$, see Fig. 1 ahead).

The components of the stress tensor, σ_{ij} and traction vector, acting on a surface with normal unit vector, n_j, $t_i = \sigma_{ij}n_j$ can be written as

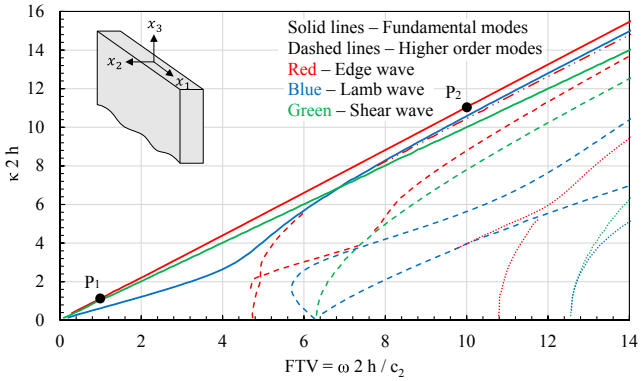

Fig. 1. Coordinate system and dispersion curves for edge waves, Lamb waves, and shear horizontal waves as presented in [27,28]. The selected frequencies (points P_1 and P_2 at $\omega\ 2h/c_2 = 0.9$ and 10, respectively) were further investigated numerically and experimentally.

$$\sigma_{ij} = \lambda\delta_{ij}\mathrm{div}\boldsymbol{u} + \mu\left(u_{i,j} + u_{j,i}\right), \tag{2}$$

where δ_{ij} is the Kronecker delta and $u_{i,j} = \partial u_i/\partial x_j$.

Wave excitation can be modelled by applying the appropriate boundary conditions at the plate edge, $x_3 = 0$,

$$\sigma_{ij}n_j = q_i(x_1, x_2, t) \tag{3}$$

The problem can be solved using the standard Laplace transform with respect to time t and Fourier transform with respect to the spatial coordinate x_1

$$\boldsymbol{U}(x_2, x_3, \omega, \xi) = \int_{-\infty}^{\infty}\int_{0}^{\infty}\boldsymbol{u}(x_1, x_2, x_3, t)e^{-\mathrm{i}(\omega t - \xi x_1)}dtdx_1 \tag{4}$$

The solution can be represented as an infinite series of wave modes, satisfying the homogeneous boundary conditions on the plate faces. In the case of symmetric excitation only symmetric modes can be excited and the solution can be represented by a superposition of the horizontally polarised shear wave modes (superscript H) and Lamb wave modes (superscript L):

$$\boldsymbol{U}(x_2, x_3, \omega, \xi) = \sum_{n=0}^{\infty} C_n^H \boldsymbol{U_n^H}(x_2)e^{-\mathrm{i}\xi_n^H x_3} + \sum_{n=0}^{\infty} C_n^L \boldsymbol{U_n^L}(x_2)e^{-\mathrm{i}\xi_n^L x_3} \tag{5}$$

where $\boldsymbol{U_n^H}$ and $\boldsymbol{U_n^L}$ are eigenfunctions, which are also related to the wavenumber, for horizontally polarised shear waves and symmetric Lamb wave modes. Thus, edge waves essentially represent a superposition of the two propagating wave modes. The eigenfunctions in Eq. (5) are explicitly provided in many articles and handbooks and will not be repeated here. C_n^H and C_n^L are unknown coefficients, which can be found from boundary conditions on the plate surfaces and edges as described previously. Several collocation techniques for the determination of these unknown coefficients have been suggested and described in a number of papers [27,28].

Fig. 1 shows the dispersion curves (solid lines) for the ES_0, shear horizontal (SH_0), and symmetric Lamb (S_0) wave modes as derived in [27] and [28] using different numerical techniques, which were applied to solve Eq. (5) with traction free boundary conditions. Higher order modes, which are not the focus of the current study, are depicted by dotted lines in Fig. 1. It can be seen that an infinite number of edge wave modes exist and these modes can propagate at various frequencies. The red curves starting from $\kappa = 0$ (κ is the wave number) corresponds to the edge resonance frequencies, which generally have complex eigenvalues [25,26].

Points P_1 and P_2 (FTV $= \omega\, 2h/c_2 = 0.9$ and 10) are investigated in the current numerical and experimental studies in order to compare with theoretical results, which have been recently published for these FTVs (frequency-thickness values) [27]. It can be observed from Fig. 1 that for low and high FTV fundamental edge wave modes, the wave speeds are very close to the corresponding shear horizontal (SH_0) and Lamb wave (S_0) modes, respectively. It is therefore a very challenging problem to effectively transfer the excitation energy from a piezoelectric transducer to a single wave mode. As a result, two or more wave modes are expected to propagate along with the fundamental edge wave mode. In addition, at relatively high FTVs (FTV > 5, see Fig. 1) multiple modes can appear and interfere with ES_0 mode, which is the focus of the current study.

3. Experimental approach

The following section describes details of the experimental approach used to study the transient behavior of the ES_0 mode over distances relevant to practical applications.

Generation of edge waves was accomplished using the wedge excitation method, which has been widely applied in many previous experimental studies for the generation of Rayleigh and Lamb wave modes [32–34]. Using this method, a longitudinal wave generated by a contact transducer is refracted into a desirable wave mode. However, as mentioned above, due to the proximity of the edge wave speed to the speeds of SH_0 and S_0 (see Fig. 1), a certain amount of the excitation energy is unavoidably transferred into these wave modes at low and high excitation frequencies, respectively.

Several materials for wedge fabrication were tested in order to find a suitable material with desirable characteristics for effective wave excitation. The wedge utilised in this study was made from an ultrahigh molecular weight polyethylene substance called 'Polystone' by the manufacturer 'Dotmar', which was selected due to its low longitudinal wave speed of approximately 2300 m/s and low attenuation characteristics. The low longitudinal speed is required to decrease the wedge angle, and subsequently, the footing area and wave propagation distance in the wedge. The wedge angle was selected to facilitate the conversion of longitudinal waves into the fundamental edge wave mode, which was found to be $\theta_w \approx 52^\circ$, see Fig. 2, based on Snell's law.

减小楔形体角度可以减小纵波速度

An oil couplant (ISO68 light motor oil) was used to acoustically bond the transducer, wedge, and specimen and enable transmission of the longitudinal wave. A range of different FTVs for the wave generation were investigated in this study. As shown in Fig. 2, the excitation wedge was located on the edge of the plate and aligned with a 3D printed fixture. This custom-made fixture ensured an even excitation energy distribution across the plate thickness. The excitation signal represented a Hann windowed sinusoidal toneburst, which was amplified to ± 200 V using a RITEC GA2500A gated amplifier for high FTV tests and a Khron-Hite 7500 amplifier for low FTV tests, respectively. The number of cycles in the excitation signal was variable and dependent on the specific experiment objective to achieve either high amplitude resolution or spatial resolution. The out-of-plane displacement at selected locations on the specimen surface was measured using a Polytec PSV-400-M2-20 scanning laser vibrometer – an instrument which has become very popular for the detection and chartacterisation of guided elastic waves [32–36]. A band pass filter appropriate for the specific excitation frequency was applied to reduce Gaussian noise. Multiple laser vibrometer scans are usually required to reduce the Gaussian noise and generation bias produced by the transducer. The laser vibrometer used in this study and experimental signal flow are both shown in Fig. 3.

The phase velocity of the ES_0 wave mode was evaluated at different FTVs, and the received signal was averaged 500 times to reduce noise as stated above. For each FTV, the arrival time of the first significant peak was identified at 11 locations along a 300 mm line segment aligned with the propagation direction. Linear regression was then applied to determine the phase speed of the ES_0 wave mode. The experimental results will be presented later in Section 5.

4. Numerical simulations of guided edge waves

In order to assist with interpretation of the experimental results, an explicit dynamics finite element model was developed using ABAQUS CAE 6-14.2 and simulated using the ABAQUS Explicit software package. Numerical results were obtained for the low (P_1) and high (P_2) FTVs as discussed previously. High FTV simulations needed a larger number of finite elements while low FTV excitation required a much longer simulation time in order to achieve a fully developed edge wave to investigate its characteristics. The geometry of the structure is shown in Fig. 4, which replicates the experimental study to be described in Section 5 in terms of the dimensionless FTV, which affects the propagation features and dispersion relationships shown in Fig. 1.

The plate thickness of 20 mm was selected for the numerical simulations to allow the FTV at points P_1 and P_2 in Fig. 1 to be investigated within a reasonable simulation time. Hann windowed sinusoidal displacement boundary conditions were applied to replicate the experimental studies. To reduce complexity associated with modeling interfaces and surface contact conditions, the initial model was created as a single solid volume, and different material properties were assigned to the wedge ($E_w = 0.9$ GPa and $\nu_w = 0.4$) and aluminum plate ($E_a = 70$

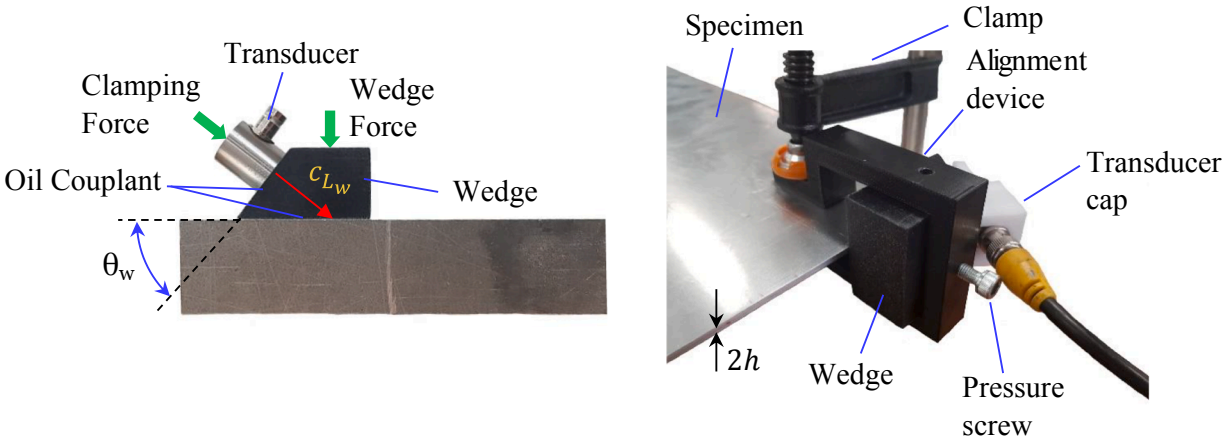

Fig. 2. Wedge generation of an edge wave in an aluminium specimen.

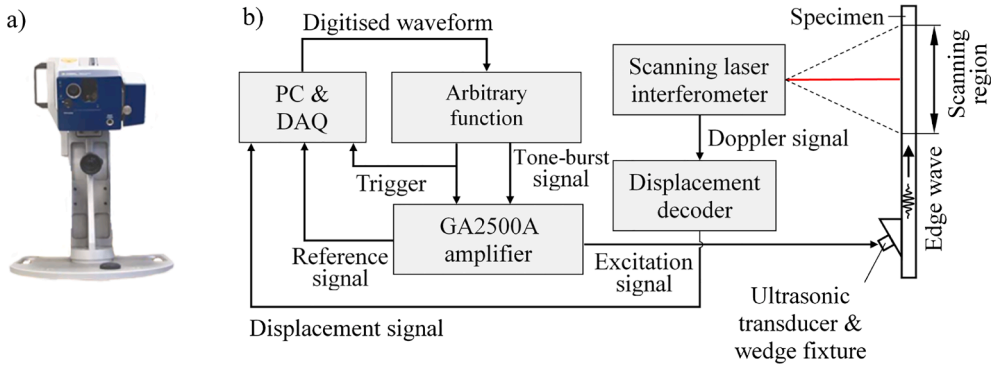

Fig. 3. (a) Polytec PSV-400-M2-20 scanning laser vibrometer used for measurement of edge waves and (b) signal flow.

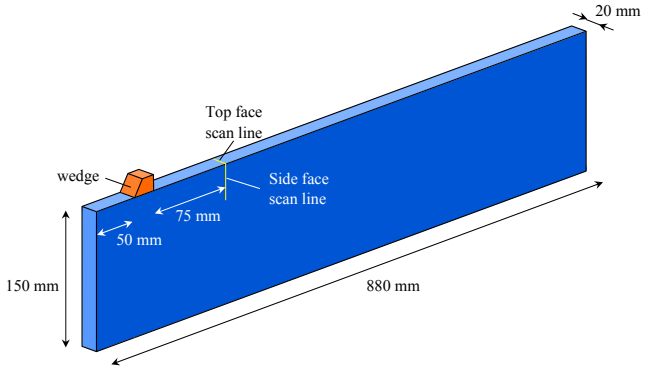

Fig. 4. Geometry of the finite element model.

GPa and $\nu_a = 0.3$), respectively. The dimensions of the 3D solid tetrahedral elements were approximately a 1 mm cube, which ensures that there are at least 10 finite elements per wavelength. Accordingly, the time-step was approximately $t_{st} \approx 82$ ns.

Fig. 5a shows the initial stage of edge wave formation at high FTVs with the wedge excitation method. It can be seen that the edge wave mode propagates at a similar speed to the fundamental symmetric Lamb wave mode. A faster wave packet, identified through mode shape analysis, is a combination of predominantly S_1 and S_2 Lamb wave modes. Although the angle of the wedge is selected to maximise the excitation amplitude of the fundamental edge wave mode, it is impossible to fully avoid the excitation of other symmetric wave modes as discussed in Section 3. The separation of the two wave packets can be

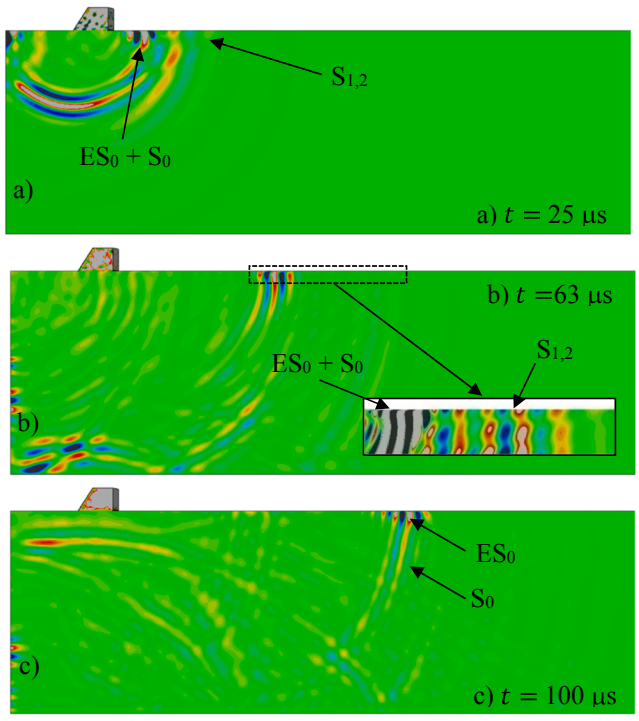

Fig. 5. u_1 displacement component along the face $x_2 = h$ (see Fig. 1 for the coordinate system) at different simulation times: 25, 63 and 100 µs.

seen in Fig. 5b. It can also be noted from FE results that the higher order Lamb wave cluster has decayed significantly, whilst the edge wave packet propagates at a relatively higher amplitude. After a sufficient time has elapsed, see Fig. 5c, the edge wave propagates along with the S_0 wave mode only, which has a significantly lower amplitude. The numerical results for the high FTV simulation correlate well with experimental observations (these will be discussed in Section 5.2), which also indicate the simultaneous excitation of the ES_0 and S_0 wave modes. The outcomes of the FE simulations for low FTVs (point P_1) will be discussed in Section 5.

5. Experimental studies and comparison with theoretical and numerical computations

The primary purpose of the experimental studies, which are described in this Section, was to evaluate the potential of the ES_0 mode for distant NDT inspections and practical applications in future SHM systems. The results presented below indicate that at low frequency-thickness values (FTV $<$ 5) edge waves can propagate over several meters without significant decay, which is very encouraging for potential practical use. There was a weak interaction between the ES_0 and SH_0 modes; the latter wave mode has very similar phase and group speeds, and it always has some presence in the elastic wave impulse generated by the wedge excitation method. It seems the interaction and interference of these wave modes is weak due to the different displacement components which are associated with propagation of these two modes.

At high frequency-thickness values, the excitation of edge waves leads to a strong presence of the fundamental Lamb wave mode, S_0, again due to the similarity between their wave speeds. In this case, the displacement components which are associated with S_0 and ES_0 are the same. As a result, a strong interaction between two modes occurs leading to an amplitude modulation, wave conversion, and strong decay. All these phenomena may restrict practical implementations of this feature-guided wave mode for NDT and SHM applications. In addition, a simple theoretical model of the amplitude modulation phenomenon was developed in this Section to verify the proposed mechanism of the wave amplitude modulation phenomenon. The model predictions are in good agreement with the experimental findings for a range of excitation frequencies.

The phase velocity of the ES_0 mode was also investigated experimentally over the low to mid excitation frequency range (FTV $<$ 7). In particular, the experimental results display a low dispersion and slight decrease in the phase speed within this range. These findings are similar to the theoretical predictions presented in [25] and other papers.

5.1. Low frequency-thickness edge waves

1D laser vibrometry was utilised to investigate the transient behavior of the fundamental edge wave mode at FTV = 0.9 (point P_1, see Fig. 1). Experimental measurements were conducted away from the wave packet formation zone (shown in Fig. 5a of the numerical study). The fundamental shear horizontal mode, SH_0, has a similar wave speed to the ES_0 mode and is therefore also inevitably generated using the wedge excitation method. However, this mode has no out-of-plane component. Therefore, the corresponding out-of-plane measurements are predominantly related to the fundamental ES_0 mode.

Initially, a long distance wave propagation test (at FTV $\approx$ 2.2) was conducted on a mild steel plate of overall length 2 m (the length was restricted by the lab space) and height 75 mm to evaluate the decay and propagation characteristics of the ES_0 wave mode (see Fig. 6). The out-of-plane displacements were recorded by the 1D laser vibrometer at two points located 500 mm and 1800 mm from the excitation wedge. From this test, it can be concluded that the fundamental edge wave mode can propagate without significant decay for up to several meters. This important finding suggests that the ES_0 wave mode at relatively low FTVs can be a promising candidate for the development of new distant damage detection techniques and non-destructive inspection methods of plate-like components with free edges. Further experimental studies were focused on the possibility of damage detection of edge defects using the ES_0 mode and standard pulse-echo method.

In the following example, see Fig. 7, a transient fundamental edge wave with FTV $\approx$ 2.2 was excited along a flange of a 125-TFB section, which is a common tapered beam widely used in construction. A crack-like defect (sharp cut) of depth 10 mm was located at a distance 625 mm from the measurement location. A clear signal reflected from the defect can be observed in Fig. 8. The amplitude of the reflection is significantly greater than the background noise, and much of the reduction in the signal amplitude can be attributed to wave conversion associated with the reflection. Based on the time-of-flight of the edge wave, the exact location of the defect can also be easily identified. Therefore, this experiment has demonstrated that the fundamental mode of edge waves has a good potential to provide a comprehensive interrogation of structures, along free surfaces, which represent the likely region for the initiation of fatigue and corrosion defects.

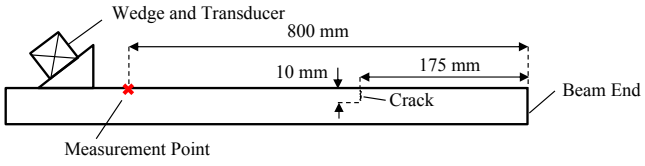

Fig. 7. Schematics of defect detection using low frequency-thickness edge waves.

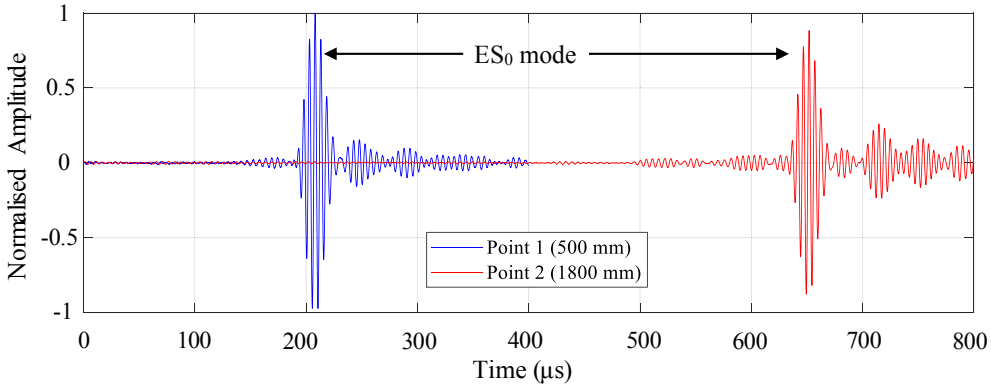

Fig. 6. ES_0 wave mode propagating in a mild steel sample of 2 m length. The amplitude decay over this distance is small, and other modes can be seen trailing the ES_0 mode.

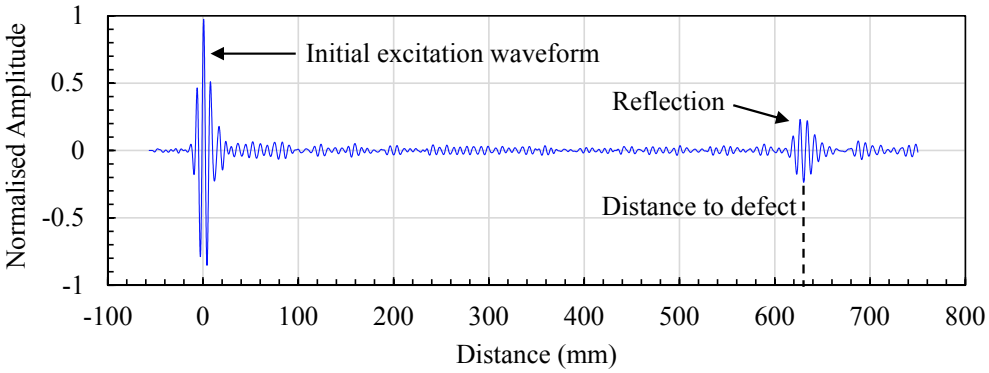

Fig. 8. Signal measurements.

5.2. High frequency-thickness edge waves

The FE study indicated that for high FTVs ($\omega 2h/c_2 > 9$) two wave modes (ES_0 and S_0) propagate with similar wave speeds, which form a wave packet at some distance from the wave excitation location, which was confirmed experimentally. The present experimental study was conducted on a 5 mm thick aluminium plate. The maximum amplitude of the out-of-plane displacements, u_3 (in the coordinate system shown in Fig. 1), of the wave packet (which was generated using the methodology outlined in Section 3) was measured at 38 locations along the top face centerline of the plate using the 1D laser vibrometer. The experimental results, which are presented as symbols in Fig. 9, demonstrate an amplitude modulation phenomenon. It is suggested that this phenomenon is associated with the interaction of the two wave modes, which have sufficiently close wave propagation speeds.

To investigate the individual properties of these wave modes, the out-of-plane displacement field can be decomposed into two decaying elastic waves with the same excitation frequency, ω, and similar wavenumbers: $\kappa_1 = \kappa_{1r} + i\kappa_{1i}$, $\kappa_2 = \kappa_{2r} + i\kappa_{2i}$ as follows:

$$u(x_1, t) = A_1 e^{i(\kappa_1 x_1 - \omega_1 t)} + A_2 e^{i(\kappa_2 x_1 - \omega_2 t)}. \quad (6)$$

A simple regression technique can be applied to obtain unknown coefficients A_1 and A_2, as well as the complex and slightly different wave numbers κ_1 and κ_2. The outcomes of the regression analysis were then fit

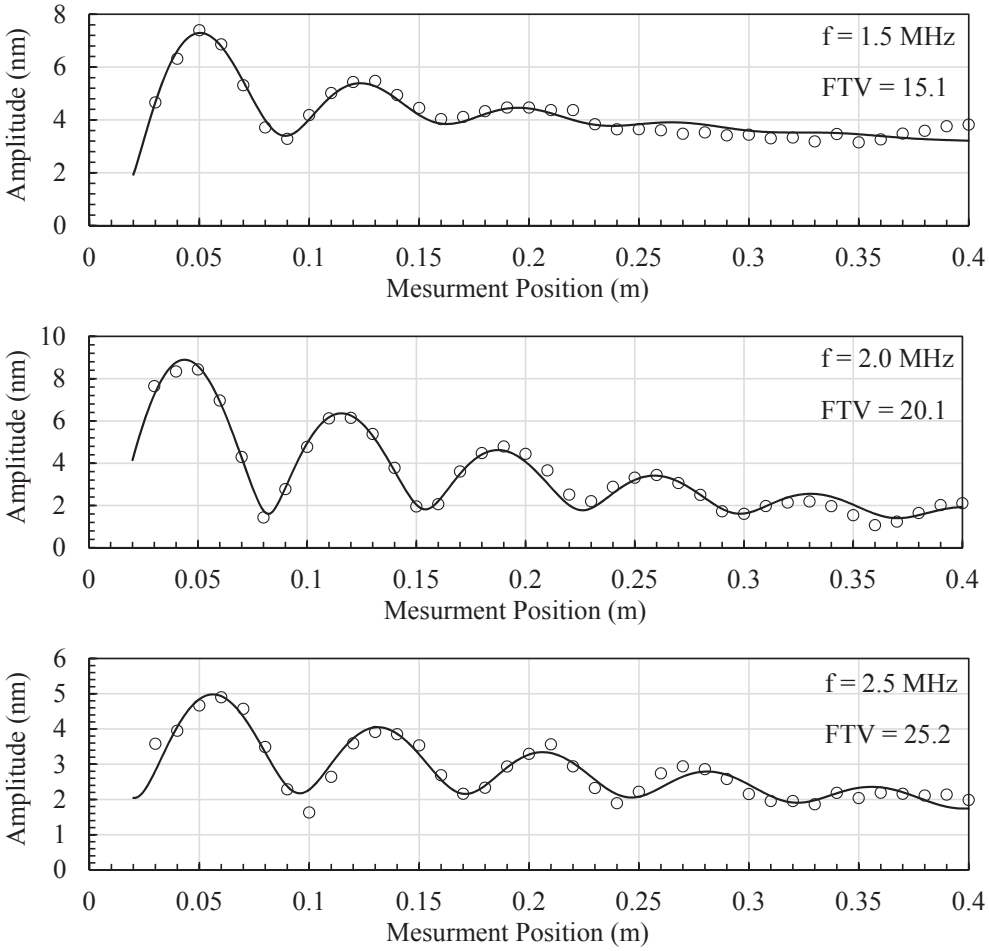

Fig. 9. Experimental results (symbols) and fitting Eq. (6) representing the superposition of two wave modes.

to determine the wavenumbers κ_1 and κ_2 and the results are shown in Fig. 9 as solid lines. A very good agreement can be noted, which supports the suggested mechanism of the amplitude modulation as well as the outcomes of the Finite Element simulations, which were presented earlier.

For excitation frequencies 1.5, 2.0, and 2.5 MHz, the corresponding difference in wavenumbers $\Delta\kappa_r = \kappa_{1r} - \kappa_{2r}$, as found from the decomposition procedure, are 86.1, 87.5, and 83.6 m^{-1} respectively. These values are very close to the theoretically predicted differences between the wave numbers of the ES_0 and S_0 modes of around 100 m^{-1} (see Fig. 1) at high FTVs (at and beyond point P_2).

The correlation between the fitting curves and experimental data is generally very good, except for the highest frequency-thickness value (FTV = 25.2). At this FTV there are some deviations, specifically at short distances. These deviations can be explained by the presence of more than two wave modes, see Fig. 1, which contribute to the out-of-plane displacements. Future studies may therefore be directed on the investigation of edge wave propagation features at high FTVs, where semi-analytical computational methodologies such as the SAFE method [12] may be applied to investigate the coupled propagation and interaction of multiple wave modes. From a practical point of view, the observed modulation phenomenon and considerable decay of the wave amplitude may significantly complicate and limit the possible practical implementations of the fundamental edge wave mode for distant inspection of damage at high FTVs or in applications, which require high defect resolution.

5.3. Further characterisation of the ES_0 mode

The out-of-plane displacements were measured on the top face and side surfaces using the 3D laser vibrometer. The experimental measurements were compared with the theoretical results of Wilde et al. [27] as well as with the current FE results for low- and high-FTV ranges. All results have been normalised with respect to the out-of-plane displacement along the centerline of the top face ($x_2 = x_3 = 0$, see Fig. 1).

Fig. 10 shows the wave mode profiles for edge waves at a low FTV. The out-of-plane displacement along the top face ($x_3 = 0$) is largely constant as predicted theoretically, numerically and measured experimentally. However, some discrepancies between all predictions can be seen in Fig. 10b. The consistent shift in the out-of-plane displacements between the experimental and theoretical results is attributed to the influence of the fundamental shear horizontal wave mode. This mode does not produce out-of-plane displacements on the top face, but has a u_2 displacement component on the side surfaces. As mentioned before,

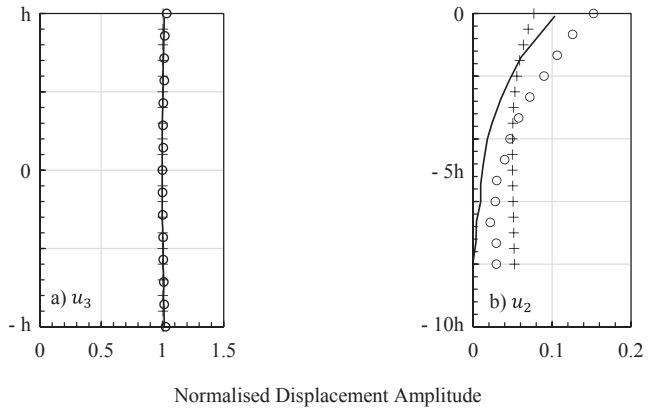

Fig. 10. Theoretical (solid lines) [27], experimental (circles) and FE (cross markers) results normalised displacements for low frequency edge waves ($\omega 2h/c_2 = 0.9$, Point 2, see Fig. 1): a) the top face $x_3 = 0$ and b) the side surface $x_2 = h$.

the SH_0 mode has a similar wave velocity to the edge wave mode, and it is virtually impossible to suppress this mode during excitation. The FE results show a significant difference, which can also be attributed to a different intensity of the SH_0 mode generated in the FE study, as well as to the finite geometry of the FE model.

A comparison between displacement mode shapes of the ES_0 wave mode calculated by the theoretical solution, finite element simulation, and experimental study at a higher FTV is shown in Figs. 11 and 12. The displacement shapes along the top face extracted from Finite Element simulations match well with the theoretical values. The small discrepancies can be attributed to the influence of other wave modes, as well as the high sensitivity of the mode shape to the excitation FTV. The out-of-plane displacements along the top face measured experimentally are presented in Fig. 11c, which are also in good agreement with both Finite Element and theoretical results. Similarly, the difference between the theoretical and experimental results at the edge of the top face are likely due to interaction with other wave modes, and the errors associated with positioning.

A good agreement between FE, theoretical, and experimental results can be observed for the higher excitation FTV on the side surfaces, see Fig. 12. The displacement obtained from FE simulations matches well with the theoretical predictions. Experimental results for the out-of-plane displacement also exhibit good agreement with the theoretical mode shape. An offset can be seen (similar to the low frequency results) which could be due to the factors mentioned above, or additionally the interaction of the wave with the S_0 mode. This error could also potentially be associated with uneven generation of the wave, as the transducer transmits more energy at the centre, which causes a flattening of the mode shape towards the side faces of the plate, or attributed to "non-ideal" geometry of the plate specimens.

These experimental results, in particular, may provide a guide regarding the most appropriate selection of sensor locations and their polarisation. For example, for relatively thick plate components locations on the top edge away from the center-line generally have higher amplitudes, see Fig. 11, and the amplitude quickly decays with the distance from the edge, see Fig. 12. These properties can be utilised to select appropriate locations for PZTs to improve the sensitivity and signal-to-noise ratio.

5.4. Measurement of the phase velocity of ES_0 waves

Fig. 13 shows the variation of the phase velocity of edge waves with FTV measured experimentally. The theoretical limit at $\omega 2h \rightarrow 0$ is the phase speed of Rayleigh waves, as it follows from several theoretical studies [25,26]. Obviously, this limit is not achievable in the current (and other) experimental study as the wavelength is limited by the dimensions of the laboratory plate sample.

The phase velocity of the edge wave initially decreases in the low to mid FTV range – a tendency, which has been reported in several theoretical studies for different Poisson's ratios [25,26]. As the changes in wave speed are relatively small, the fundamental edge wave mode can be considered as weakly dispersive, which is important for the development of defect detection and damage evaluation procedures, as it allows the defect triangulation using a simple time-of-flight approach (see Section 5.1). This low dispersion feature may also allow for the application of non-linear techniques for damage diagnostics, e.g. based on higher harmonic generation, which require phase and group velocity matching [36–39]. However, the non-linear aspects of ES_0 wave mode propagation are not within the scope of the current study, but may form the basis for future research along with studies focusing on propagation of edge waves along curved wave-guides or plates with round edges.

6. Conclusion

This article presents a detailed experimental investigation of the propagation of the fundamental edge wave mode, ES_0, over long

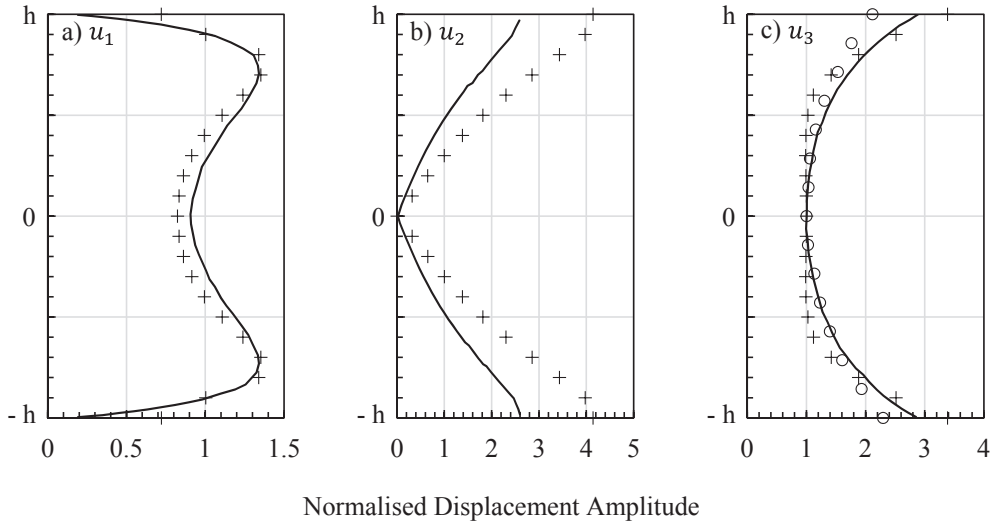

Fig. 11. Theoretical (solid lines) [27], experimental (circles) and finite element (cross markers) out-of-plane displacements along the top face $x_3 = 0$ for a high frequency edge wave at $\omega 2h/c_2 = 10$ in three directions.

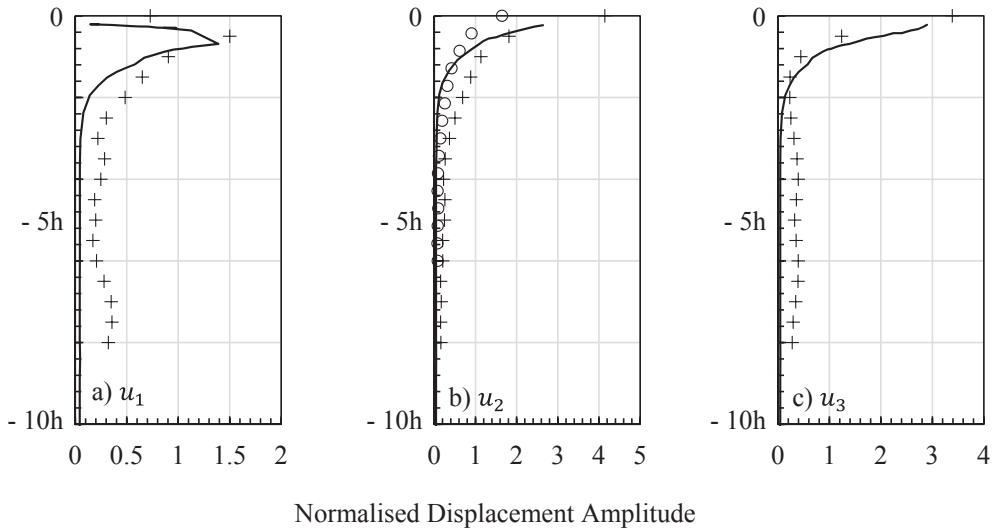

Fig. 12. Theoretical (solid lines) [27], present experimental (circles) and finite element (cross markers) out-of-plane displacements along the side face $x_2 = h$ for a high frequency edge wave at $\omega 2h/c_2 = 10$ in three directions.

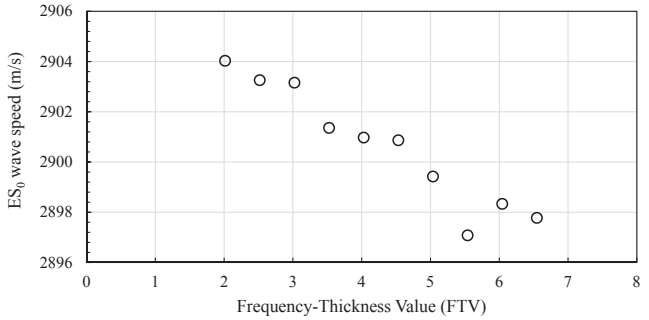

Fig. 13. Phase velocity of the fundamental edge wave mode for a 5 mm thick aluminium plate.

(practical) distances with a focus on the demonstration of its potential for use in NDE and SHM. The wedge excitation method was successfully applied to generate the ES_0 mode at low and high frequency-thickness values (FTVs). Due to the close proximity of the wave speed of ES_0 to SH_0 and S_0, these fundamental modes were also generated along with the edge wave for low and high FTVs, respectively. For low frequencies, it was found that the SH_0 mode does not affect the normal (out-of-plane) displacements at the top face, and the excited waves are capable of propagating long distances without significant attenuation. The conducted feasibility study revealed a great potential for the use of these feature-guided waves for damage detection and monitoring.

For high FTVs, the simultaneous excitation of the ES_0 mode and S_0 mode leads to an amplitude modulation behavior. The amplitude modulation phenomenon was modelled theoretically, and a good agreement between the experimental results and theoretical predictions was seen. In addition, a relatively high-energy dispersion and signal amplitude decay were found, which are in a general agreement with analytical predictions of several theoretical studies.

It was also demonstrated that a high fidelity transient FE method could be used to investigate the propagation of the fundamental mode of edge waves. This numerical method could potentially be an alternative to experimental studies or theoretical solutions, which are tedious and difficult to derive for this type of guided waves. The differences between

the current FE and experimental results, as well as the published theoretical results, are largely attributed to the effects of the interaction with SH_0, S_0 and higher order wave modes, which are difficult to control during excitation in experiments.

In terms of the potential applications of edge waves for defect detection, the fundamental mode of edge waves at relatively low FTVs (FTV < 5) demonstrates a great potential for long range inspections. ES_0 mode can propagate without significant decay (for up to 2 m in a laboratory environment), however the defect resolution in this case may be limited due to the relatively large wavelength. In contrast, ES_0 mode at FTVs should provide a better defect resolution, but will not propagate as far. Another observed phenomenon is an amplitude modulation at high FTVs, which may affect signal processing and interpretation. These limiting factors should be taken into consideration in the development of practical damage detection systems for NDE and SHM. Across low to mid excitation frequencies the fundamental edge wave mode was found to be weakly dispersive in terms of the phase and group speeds, which is also important for signal processing and defect localisation procedures. Future studies on edge waves could be focused on the effect of the local geometry, curvature of the waveguide, on the study of the reflection coefficient and the relationship between the wavelength of the ES_0 mode and the detectable size of defect. As such, this paper provides a guide for future theoretical and experimental studies, as well as for practical implementation of the feature-guided ES_0 wave mode for the development of new distant NDT inspection techniques and SHM systems.

CRediT authorship contribution statement

James M. Hughes: Conceptualization, Methodology, Software, Formal analysis, Investigation, Data curation, Writing - original draft, Visualization. **Munawwar Mohabuth:** Methodology, Software, Validation, Formal analysis, Investigation, Resources, Writing - review & editing. **Andrei Kotousov:** Conceptualization, Methodology, Formal analysis, Writing - review & editing, Supervision, Project administration, Funding acquisition. **Ching-Tai Ng:** Conceptualization, Writing - review & editing, Supervision, Funding acquisition.

Declaration of Competing Interest

None.

Acknowledgments

This work was supported by the Australian Research Council through DP160102233, LE170100079, DP200102300 and the Australian Government Research Training Program Scholarship. Their support is greatly appreciated.

References

[1] D.N. Alleyne, B. Pavlakovic, M.J.S. Lowe, P. Cawley, Rapid, long range inspection of chemical plant pipework using guided waves, Insight 43 (2001) 93–101, https://doi.org/10.1063/1.1373757.
[2] L.R. Rose, A baseline and vision of ultrasonic guided wave inspection potential, J. Pressure Vessel Technol. 124 (3) (2002) 273–282, https://doi.org/10.1115/1.1491272.
[3] P. Aryan, A. Kotousov, C.T. Ng, B. Cazzolato, A baseline-free and non-contact method for detection and imaging of structural damage using 3D laser vibrometry, Struct. Control Health Monitor. 24 (4) (2017), e1894, https://doi.org/10.1002/stc.1894.
[4] P. Aryan, A. Kotousov, C.T. Ng, S. Wildy, Reconstruction of baseline time-trace under changing environmental and operational conditions, Smart Mater. Struct. 25 (2016), 035018, https://doi.org/10.1088/0964-1726/25/3/035018.
[5] H. Sohn, Reference-free crack detection under varying temperature, KSCE J. Civ. Eng. 15 (8) (2011) 1395–1404, https://doi.org/10.1007/s12205-011-1271-0.
[6] G. Konstantinidis, B.W. Drinkwater, P.D. Wilcox, The temperature stability of guided wave structural health monitoring systems, Smart Mater. Struct. 15 (2006) 967–976, https://doi.org/10.1088/0964-1726/15/4/010.
[7] M. Mohabuth, A. Kotousov, C.T. Ng, Effect of uniaxial stress on the propagation of higher-order Lamb wave modes, Int. J. Non Linear Mech. 86 (2016) 104–111, https://doi.org/10.1016/j.ijnonlinmec.2016.08.006.
[8] M. Mohabuth, A. Kotousov, C.T. Ng, L.R.F. Rose, Implication of changing loading conditions on structural health monitoring utilizing guided wave, Smart Mater. Struct. 27 (2018), 025003, https://doi.org/10.1088/1361-665X/aa9f89.
[9] B. Vien, L. Rose, W. Chiu, Experimental and computational studies on the scattering of an edge-guidedwave by a hidden crack on a racecourse shaped hole, Materials 10 (2017) 732, https://doi.org/10.3390/ma10070732.
[10] H. Mohseni, C.T. Ng, Rayleigh wave propagation and scattering characteristics at debondings in fibre-reinforced polymer-retrofitted concrete structures, Struct. Health Monitor. 18 (1) (2019) 303–317, https://doi.org/10.1177/1475921718754371.
[11] Y. Yang, C.T. Ng, A. Kotousov, Bolted joint integrity monitoring with second harmonic generated by guided waves, Struct. Health Monitor. 18 (1) (2019) 193–204, https://doi.org/10.1177/1475921718814399.
[12] Z. Yang, K. Liu, K. Zhou, Yu. Liang, J. Zhang, Y. Zheng, D. Gao, S. Ma, Z. Wu, Investigation of thermo-acoustoelastic guided waves by semi-analytical finite element method, Ultrasonics 106 (2020), 106141.
[13] J.B. Lawrie, J.D. Kaplunov, Edge waves and resonance on elastic structures: an overview, Math. Mech. Solid 17 (2012) 4–16, https://doi.org/10.1177/1081286511412281.
[14] Z. Fan, M. Castaings, M.J.S. Lowe, C. Biateau, P. Froome, Feature-guided waves for monitoring adhesive shear modulus in bonded stiffeners, NDT&E Int. 54 (2013) 96–102, https://doi.org/10.1016/j.ndteint.2012.12.006.
[15] X. Yu, M. Ratassepp, Z. Fan, Damage detection in quasi-isotropic composite bends using ultrasonic feature guided waves, Compos. Sci. Technol. 141 (2017) 120–129, https://doi.org/10.1016/j.compscitech.2017.01.011.
[16] Z. Fan, M.J.S. Lowe, Elastic waves guided by a welded joint in a plate, Proc. R. Soc. A. 465 (2009) 2053–2068, https://doi.org/10.1098/rspa.2009.0010.
[17] X. Yu, P. Zhu, J. Xiao, Z. Fan, Detection of damage in welded joints using higher order feature guided ultrasonic waves, Mech. Syst. Sig. Process. 126 (2019) 176–192, https://doi.org/10.1016/j.ymssp.2019.02.026.
[18] X. Yu, Z. Fan, M. Castaings, C. Biateau, Feature guided wave inspection of bond line defects between a stiffener and a composite plate, NDT&E Int. 89 (2017) 44–55, https://doi.org/10.1016/j.ndteint.2017.03.008.
[19] V.V. Krylov, R. E.T.B. Winward, Experimental investigation of the acoustic black hole effect for flexural waves in tapered plates, J. Sound Vib., 300 (1–2) 43-49.
[20] M.I. Chen, S.-P. Tesng, P.-Y. Lo, C.-H. Yang, Characterization of wedge waves propagating along wedge tips with defects, Ultrasonics 82 (2018) 289–297, https://doi.org/10.1016/j.ultras.2017.09.010.
[21] J. Corcoran, E. Leinov, A. Jeketo, M.J.S. Lowe, A guided wave inspection technique for wedge features, IEEE Trans. Ultrason. Ferroelectr. Freq. Control 67 (5) (2020) 997–1008.
[22] M. de Billy, Acoustic technique applied to the measurement of the free edge wave velocity, Ultrasonics 34 (1996) 611–619.
[23] M. de Billy, A.C. Hladky-Hennion, The effect of imperfections on acoustic pave propagation along a wedge waveguide, Ultrasonics 37 (1999) 413–416.
[24] J.W.S. Rayleigh, On waves propagated along the plane surface of an elastic solid, Proc. Lond. Math. Soc. S1–17 (1) (1885) 4–11, https://doi.org/10.1112/plms/s1-17.1.4.
[25] V. Zernov, J. Kaplunov, Three dimensional edge-waves in plates, Proc. R. Soc. Lond. A464 (2008) 301–318, https://doi.org/10.1098/rspa.2007.0159.
[26] J. Kaplunov, D.A. Prikazchikov, G.A. Rogerson, On three-dimensional edge waves in semi-infinite isotropic plates subject to mixed face boundary conditions, J. Acoust. Soc. Am. 118 (2006) 2975-2983. DOI: 10.1121/1.2062487.
[27] M.V. Wilde, M.V. Golub, A.A. Eremin, Experimental and theoretical investigation of transient edge waves excited by a piezoelectric transducer bonded to the edge of a thick elastic plate, J. Sound Vib. 44 (2019) 26–49, https://doi.org/10.1016/j.jsv.2018.10.015.
[28] F. Feng, Z. Shen, J. Shen, Edge waves in a 3D plate: Two solutions based on plate mode matching, Math. Mech. Solids 22 (2016) 2043–2052, https://doi.org/10.1177/1081286516657682.
[29] E.A.G. Shaw, On the resonant vibrations of thick barium titanate disks, J. Acoust. Soc. Am. 28 (1956) 38–50, https://doi.org/10.1121/1.1908218.
[30] D.G. Gazis, R.D. Mindlin, Extensional vibrations and waves in a circular disk and a semiinfinite plate, J. Appl. Mech. 27 (1960) 541–547, https://doi.org/10.1115/1.3644037.
[31] A.J. Croxford, P.D. Wilcox, B.W. Drinkwater, G. Konstantinidis, Strategies for guidedwave structural health monitoring, Proc. R. Soc. A 463 (2007) 2961–2981.
[32] J.M. Hughes, J. Vidler, C.-T. Ng, A. Khanna, M. Mohabuth, L.F.R. Rose, A. Kotousov, Comparative evaluation of in situ stress monitoring with Rayleigh waves, Struct. Health Monitor. Special Issue: Real World Appl. SHM (2018) 1–11, https://doi.org/10.1177/1475921718798146.
[33] J. Hermann, Generation and detection of higher order harmonics in Rayleigh waves using laser ultrasound. Master's Thesis, Georgia Institute of Technology, Atlanta, 2005.
[34] W.J. Staszewski, B.C. Lee, L. Mallet, F. Scarpa, Structural health monitoring using scanning laser vibrometry: I. Lamb wave sensing, Smart Mater. Struct. 13 (2004) 251–260, https://doi.org/10.1088/0964-1726/13/2/002.
[35] L. Mallet, B.C. Lee, W.J. Stazewski, F. Scarpa, Structural health monitoring using scanning laser vibrometry: II. Lamb waves for damage detection, Smart Mater. Struct. 13 (2004) 261–269, https://doi.org/10.1088/0964-1726/13/2/003.
[36] K.H. Matlack, J.-Y. Kim, L.J. Jacobs, J. Qu, Review of Second Harmonic Generation Measurement Techniques for Material State Determination in Metals, J. Nondestruct. Eval. (34):273 (2015), https://doi.org/10.1007/s10921-014-0273-5.

[37] A.N. Norris, V.V. Krylov, I.D. Abrahams, Flexural edge waves and Comments on "A new bending wave solution for the classical plate equation", J. Acoust. Soc. Am. 107 (2000) 1781–1784, https://doi.org/10.1121/1.428457.
[38] J.M. Hughes, A. Kotousov, C.-T. Ng, Generation of Higher Harmonics with the Fundamental Edge Wave Mode, Appl. Phys. Lett. 116 (2020), 101904, https://doi.org/10.1063/1.5142416.
[39] S. Zhang, X. Li, H. Jeong, H. Hu, Experimental investigation of material nonlinearity using the Rayleigh surface waves excited and detected by angle beam wedge transducers, Ultrasonics 89 (2018) 118–125.